

1
2
3
4
5
6
7
8
9
10
11
12
13
14
15
16
17
18
19
20
21
22
23
24
25
26
27
28
29
30
31
32
33
34
35
36
37
38
39
40
41
42
43
44
45
46
47
48
49
50
51
52
53
54
55
56
57
58
59
60
61
62

63
64
65
66
67
68
69
70
71
72
73
74
75
76
77
78
79
80
81
82
83
84
85
86
87
88
89
90
91
92
93
94
95
96
97
98
99
100
101
102
103
104
105
106
107
108
109
110
111
112
113
114
115
116
117
118
119
120
121
122
123
124

Supplementary Information for

Altered conformational landscape and dimerization dependency underpins the activation of EGFR by α C- β 4 loop insertion mutations

Zheng Ruan and Natarajan Kannan

To whom correspondence should be addressed:

Natarajan Kannan

E-mail: nkannan@uga.edu

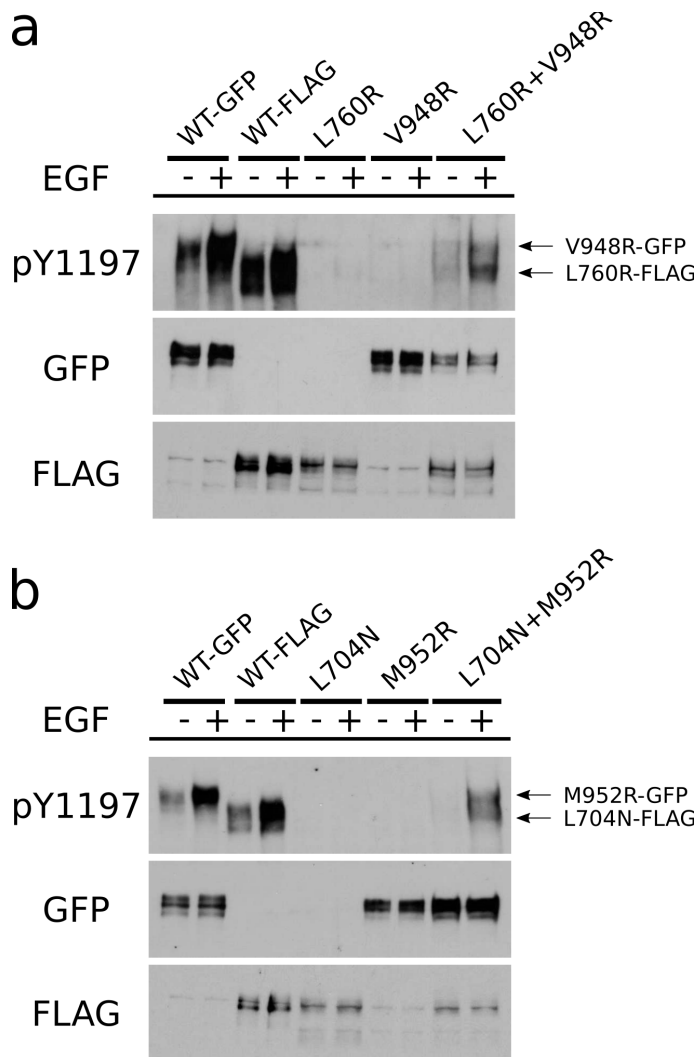
This PDF file includes:

- Figs. S1 to S10
- Tables S1 to S3
- Caption for Database S1

Other supplementary materials for this manuscript include the following:

- Database S1

125
126
127
128
129
130
131
132
133
134
135
136
137
138
139
140
141
142
143
144
145
146
147
148
149
150
151
152
153
154
155
156
157
158
159
160
161
162
163
164
165
166
167
168
169
170
171
172
173
174
175
176
177
178
179
180
181
182
183
184
185
186



187
188
189
190
191
192
193
194
195
196
197
198
199
200
201
202
203
204
205
206
207
208
209
210
211
212
213
214
215
216
217
218
219
220
221
222
223
224
225
226
227
228
229
230
231
232
233
234
235
236
237
238
239
240
241
242
243
244
245
246
247
248

Fig. S1. Western blot analysis of WT EGFR with N-lobe (L760R and L704N) and C-lobe (V948R and M952R) dimerization deficient mutations. 5% SDS-PAGE is used to analyze Y1197 phosphorylation. The bands corresponding to GFP and FLAG tagged EGFR are labeled by the arrows in (a) and (b).

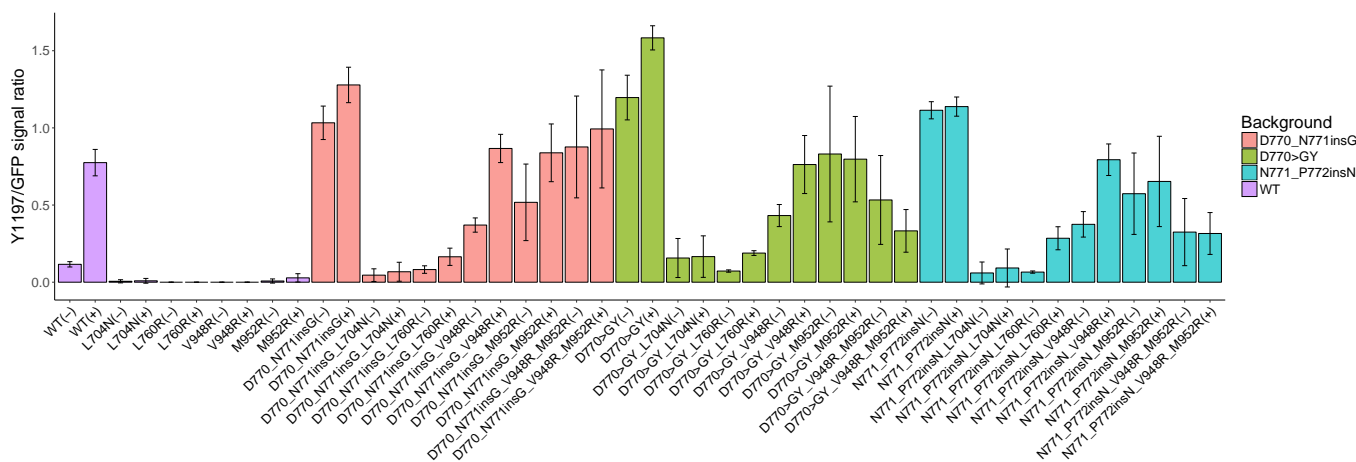


Fig. S2. Densitometry analysis of the Western Blotting results in Fig. 3a. Error bar represents standard error (SE) of 3-5 independent experiments.

249
250
251
252
253
254
255
256
257
258
259
260
261
262
263
264
265
266
267
268
269
270
271
272
273
274
275
276
277
278
279
280
281
282
283
284
285
286
287
288
289
290
291
292
293
294
295
296
297
298
299
300
301
302
303
304
305
306
307
308
309
310

311
312
313
314
315
316
317
318
319
320
321
322
323
324
325
326
327
328
329
330
331
332
333
334
335
336
337
338
339
340
341
342
343
344
345
346
347
348
349
350
351
352
353
354
355
356
357
358
359
360
361
362
363
364
365
366
367
368
369
370
371
372

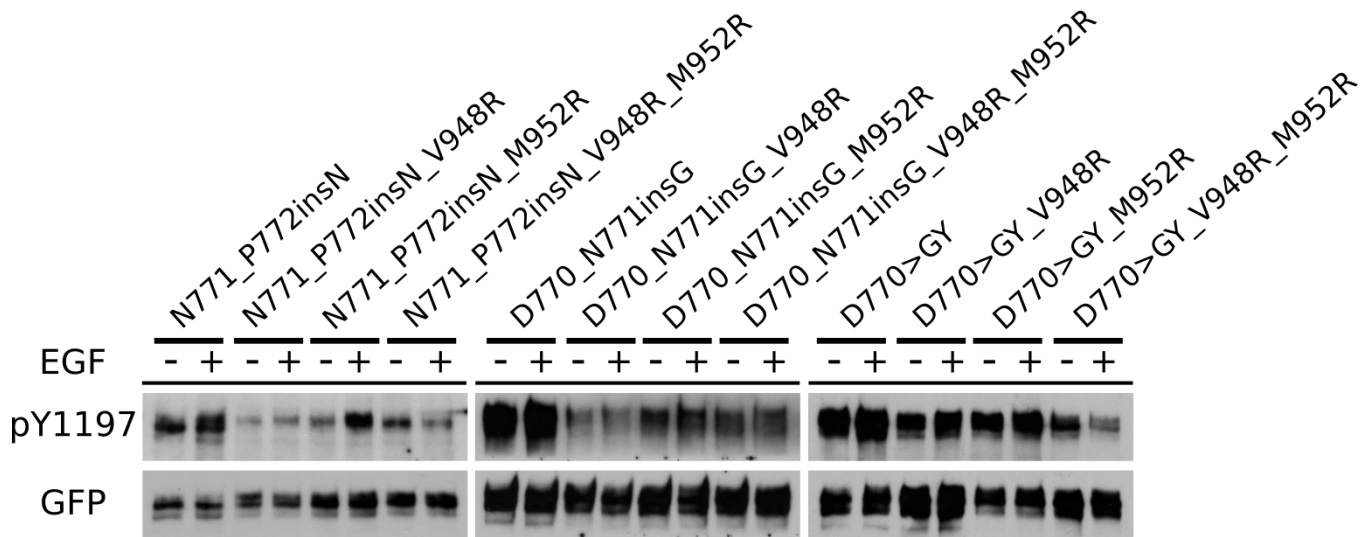


Fig. S3. Activating insertion mutations are tolerant to C-lobe dimerization-deficient mutations. EGFR C-lobe dimerization-deficient mutations, V948R or M952R or V948R+M952R, are introduced to N771_P772insN, D770_N771insG, and D770>GY mutants background. Auto-phosphorylation of Y1197 is probed through phospho-specific antibody. The total expression of the designated constructs is detected using GFP antibody.

373
374
375
376
377
378
379
380
381
382
383
384
385
386
387
388
389
390
391
392
393
394
395
396
397
398
399
400
401
402
403
404
405
406
407
408
409
410
411
412
413
414
415
416
417
418
419
420
421
422
423
424
425
426
427
428
429
430
431
432
433
434

435
436
437
438
439
440
441
442
443
444
445
446
447
448
449
450
451
452
453
454
455
456
457
458
459
460
461
462
463
464
465
466
467
468
469
470
471
472
473
474
475
476
477
478
479
480
481
482
483
484
485
486
487
488
489
490
491
492
493
494
495
496

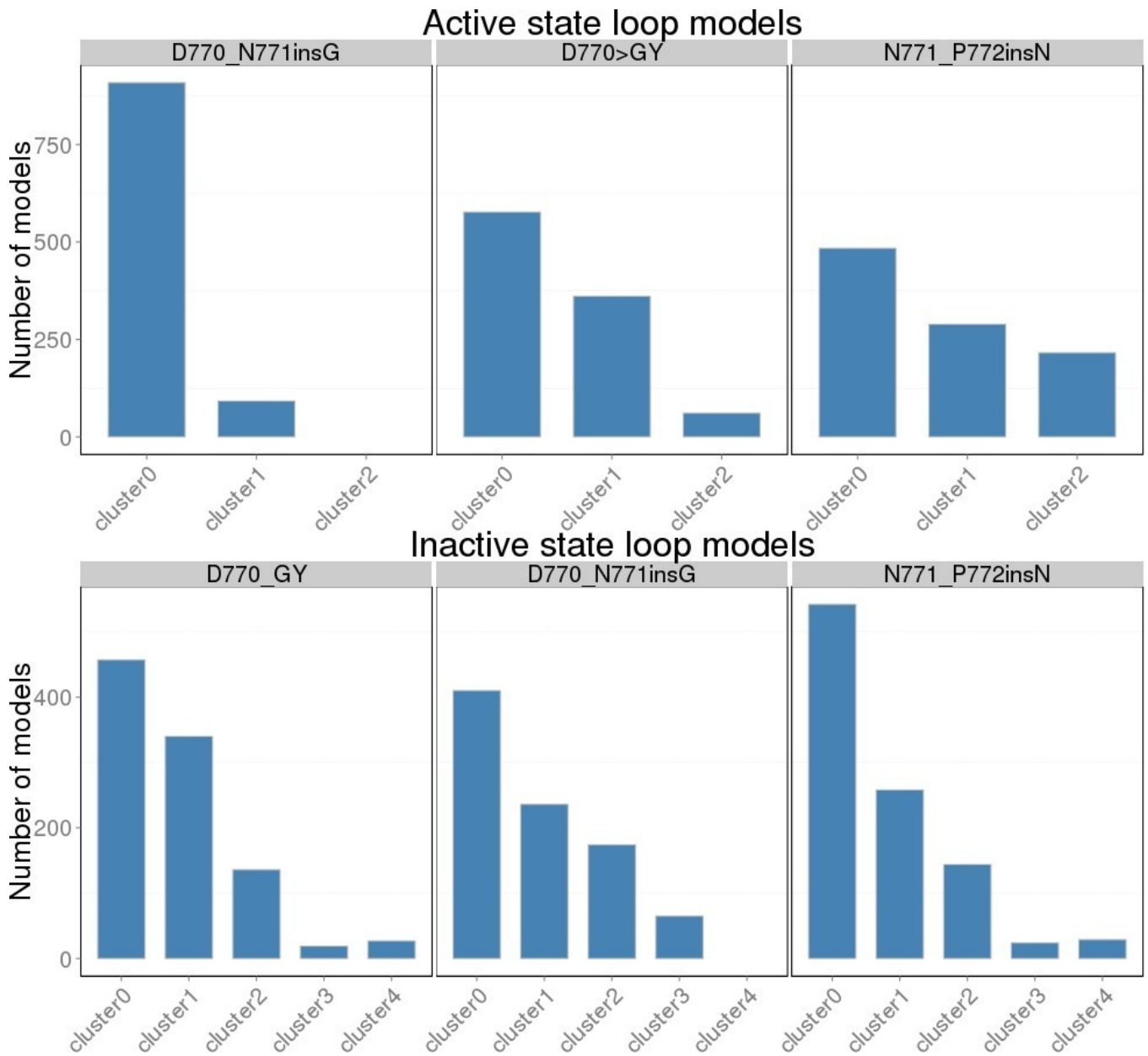


Fig. S4. The number of clusters identified from 1000 α C- β 4 loop insertion mutation models in active/inactive states.

497
498
499
500
501
502
503
504
505
506
507
508
509
510
511
512
513
514
515
516
517
518
519
520
521
522
523
524
525
526
527
528
529
530
531
532
533
534
535
536
537
538
539
540
541
542
543
544
545
546
547
548
549
550
551
552
553
554
555
556
557
558

559
560
561
562
563
564
565
566
567
568
569
570
571
572
573
574
575
576
577
578
579
580
581
582
583
584
585
586
587
588
589
590
591
592
593
594
595
596
597
598
599
600
601
602
603
604
605
606
607
608
609
610
611
612
613
614
615
616
617
618
619
620

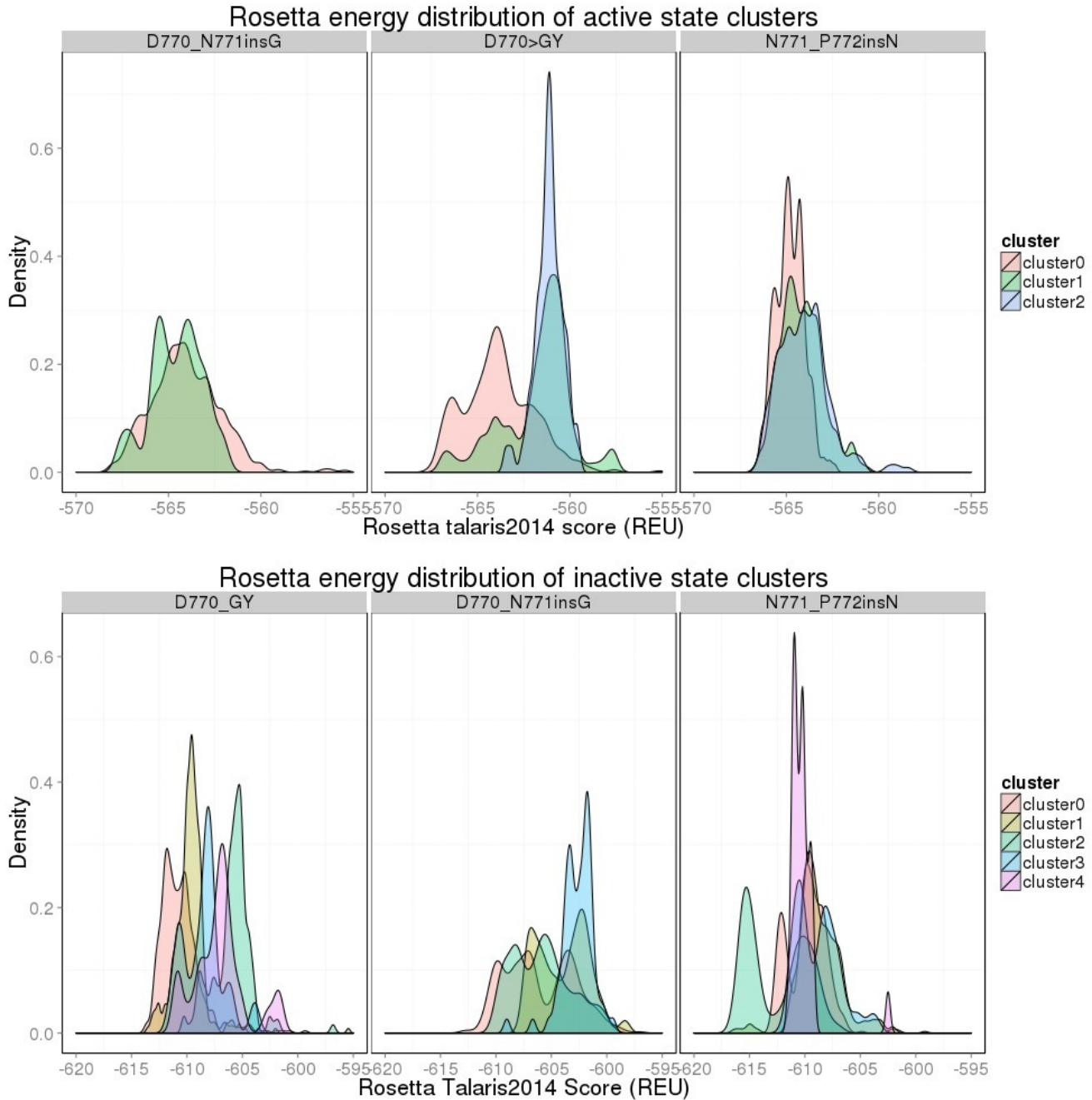


Fig. S5. The rosetta energy distribution of each cluster identified in Fig. S4.

621
622
623
624
625
626
627
628
629
630
631
632
633
634
635
636
637
638
639
640
641
642
643
644
645
646
647
648
649
650
651
652
653
654
655
656
657
658
659
660
661
662
663
664
665
666
667
668
669
670
671
672
673
674
675
676
677
678
679
680
681
682

683
684
685
686
687
688
689
690
691
692
693
694
695
696
697
698
699
700
701
702
703
704
705
706
707
708
709
710
711
712
713
714
715
716
717
718
719
720
721
722
723
724
725
726
727
728
729
730
731
732
733
734
735
736
737
738
739
740
741
742
743
744

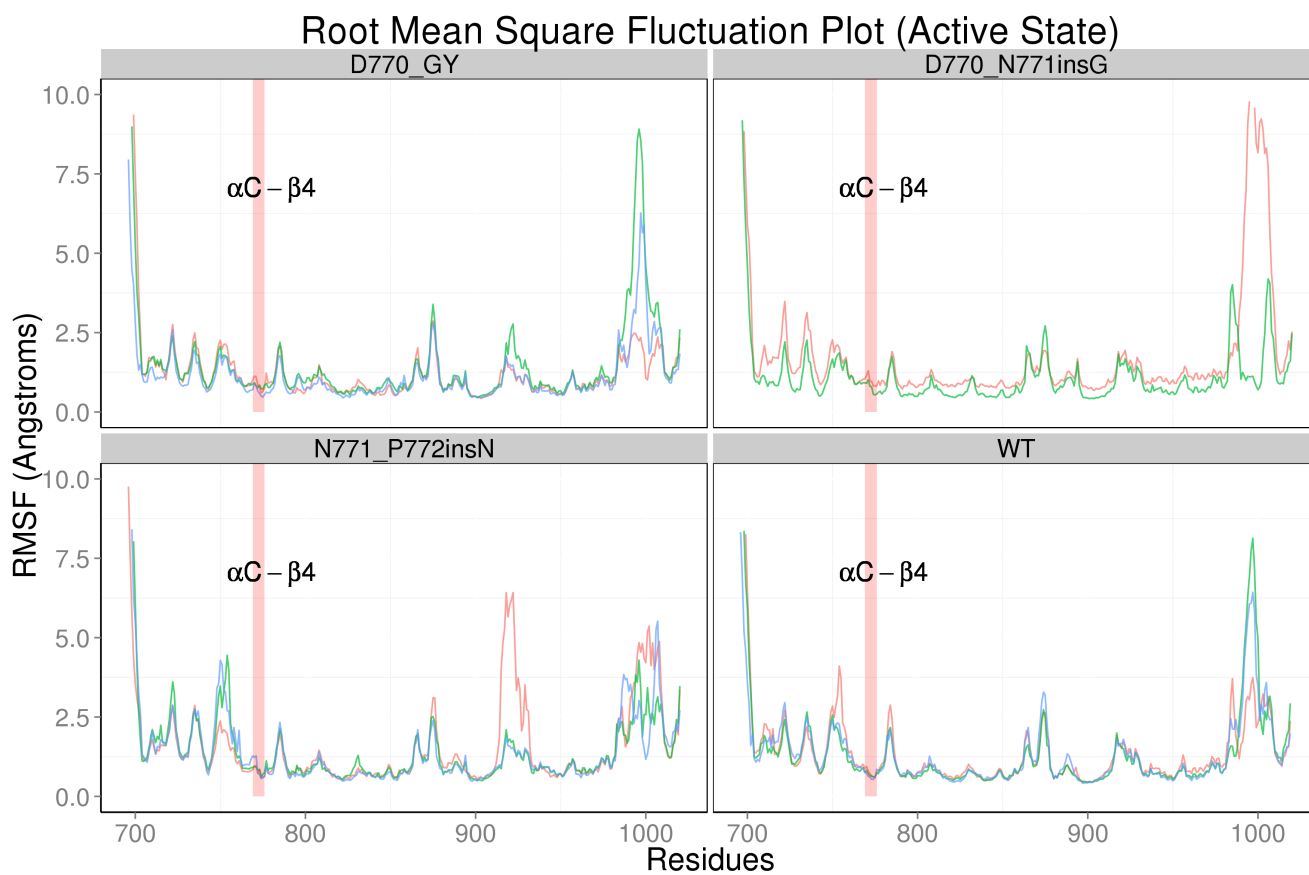


Fig. S6. Root mean square fluctuation (RMSF) plot of WT EGFR and three activating insertion mutations in the active state. Residues correspond to the α C- β 4 loop are highlighted in red.

745
746
747
748
749
750
751
752
753
754
755
756
757
758
759
760
761
762
763
764
765
766
767
768
769
770
771
772
773
774
775
776
777
778
779
780
781
782
783
784
785
786
787
788
789
790
791
792
793
794
795
796
797
798
799
800
801
802
803
804
805
806

807
808
809
810
811
812
813
814
815
816
817
818
819
820
821
822
823
824
825
826
827
828
829
830
831
832
833
834
835
836
837
838
839
840
841
842
843
844
845
846
847
848
849
850
851
852
853
854
855
856
857
858
859
860
861
862
863
864
865
866
867
868

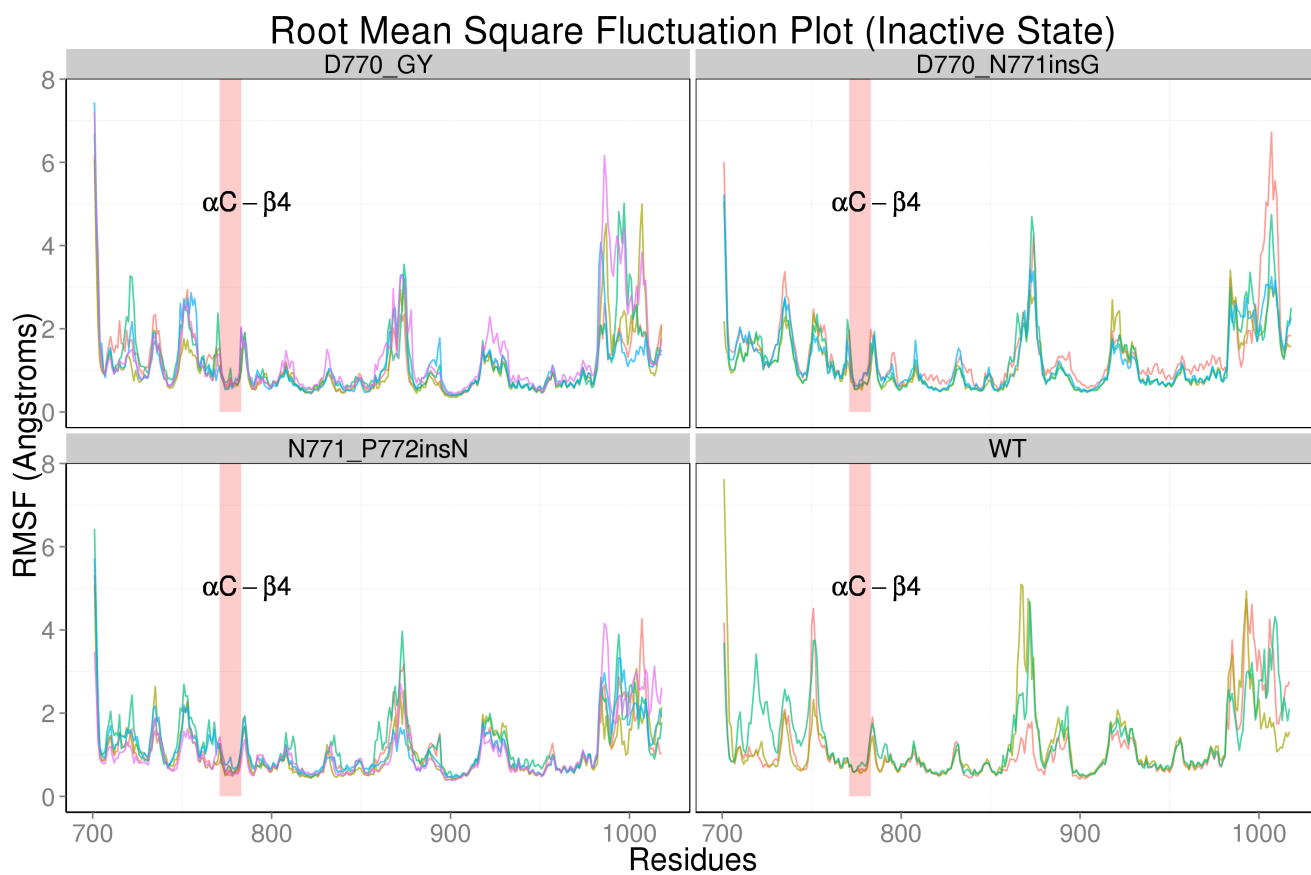


Fig. S7. Root mean square fluctuation (RMSF) plot of EGFR and three activating insertion mutations in the inactive state. Residues correspond to the α C- β 4 loop are highlighted in red.

869
870
871
872
873
874
875
876
877
878
879
880
881
882
883
884
885
886
887
888
889
890
891
892
893
894
895
896
897
898
899
900
901
902
903
904
905
906
907
908
909
910
911
912
913
914
915
916
917
918
919
920
921
922
923
924
925
926
927
928
929
930

931
932
933
934
935
936
937
938
939
940
941
942
943
944
945
946
947
948
949
950
951
952
953
954
955
956
957
958
959
960
961
962
963
964
965
966
967
968
969
970
971
972
973
974
975
976
977
978
979
980
981
982
983
984
985
986
987
988
989
990
991
992

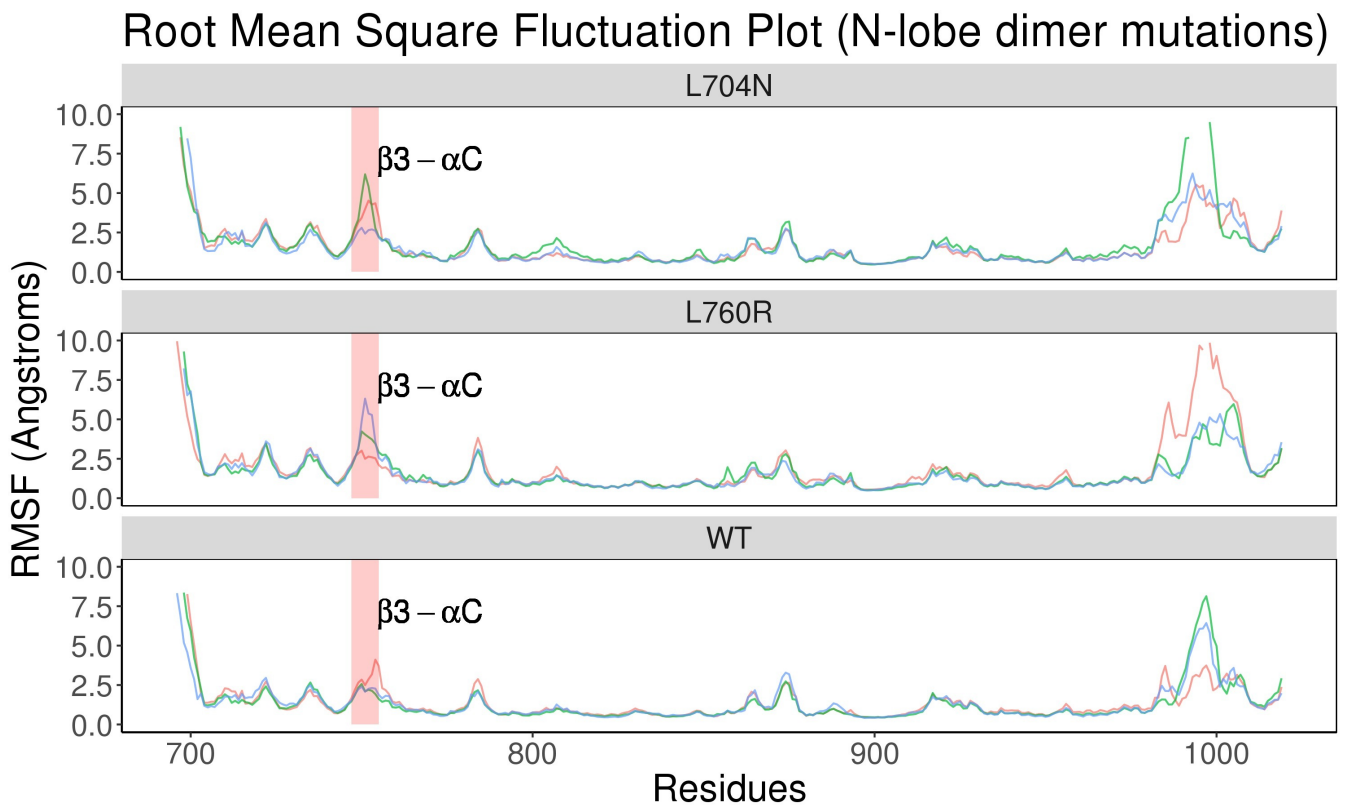


Fig. S8. Root mean square fluctuation (RMSF) plot of EGFR and two N-lobe dimerization deficient mutations. Residues correspond to the $\beta 3 - \alpha C$ loop are highlighted in red.

993
994
995
996
997
998
999
1000
1001
1002
1003
1004
1005
1006
1007
1008
1009
1010
1011
1012
1013
1014
1015
1016
1017
1018
1019
1020
1021
1022
1023
1024
1025
1026
1027
1028
1029
1030
1031
1032
1033
1034
1035
1036
1037
1038
1039
1040
1041
1042
1043
1044
1045
1046
1047
1048
1049
1050
1051
1052
1053
1054

1055
1056
1057
1058
1059
1060
1061
1062
1063
1064
1065
1066
1067
1068
1069
1070
1071
1072
1073
1074
1075
1076
1077
1078
1079
1080
1081
1082
1083
1084
1085
1086
1087
1088
1089
1090
1091
1092
1093
1094
1095
1096
1097
1098
1099
1100
1101
1102
1103
1104
1105
1106
1107
1108
1109
1110
1111
1112
1113
1114
1115
1116

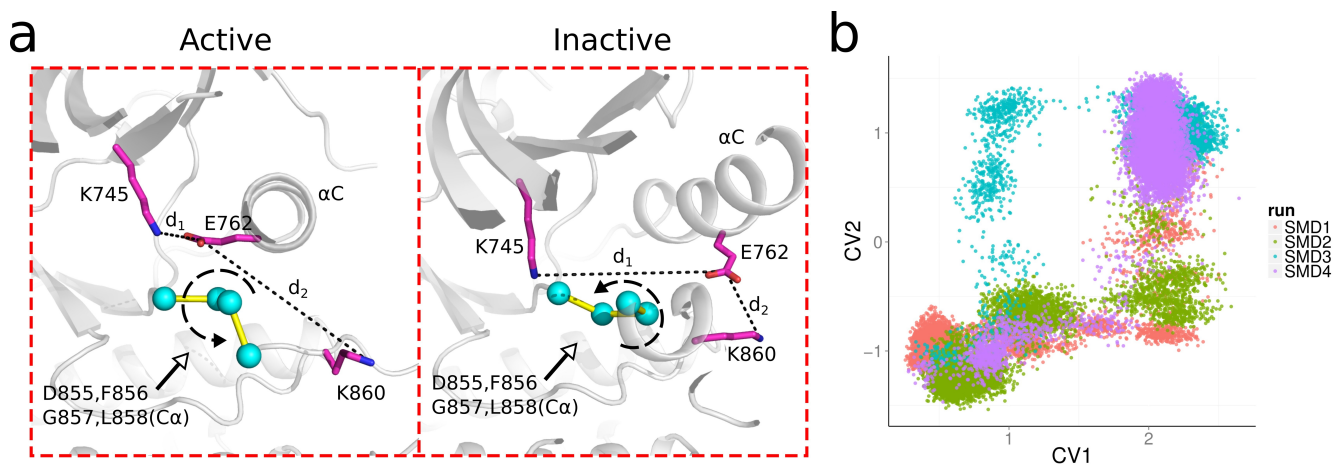


Fig. S9. a) The two collective variables used in our US simulation are shown in the active and inactive structures of EGFR. CV1: the dihedral angle of $C\alpha[D855]-C\alpha[F856]-C\alpha[G857]-C\alpha[L858]$. CV2: $d_2[E762-K860]-d_1[K745-E762]$. b) Visualization of four independent steered MD simulation through CV1 and CV2.

1117
1118
1119
1120
1121
1122
1123
1124
1125
1126
1127
1128
1129
1130
1131
1132
1133
1134
1135
1136
1137
1138
1139
1140
1141
1142
1143
1144
1145
1146
1147
1148
1149
1150
1151
1152
1153
1154
1155
1156
1157
1158
1159
1160
1161
1162
1163
1164
1165
1166
1167
1168
1169
1170
1171
1172
1173
1174
1175
1176
1177
1178

1179
1180
1181
1182
1183
1184
1185
1186
1187
1188
1189
1190
1191
1192
1193
1194
1195
1196
1197
1198
1199
1200
1201
1202
1203
1204
1205
1206
1207
1208
1209
1210
1211
1212
1213
1214
1215
1216
1217
1218
1219
1220
1221
1222
1223
1224
1225
1226
1227
1228
1229
1230
1231
1232
1233
1234
1235
1236
1237
1238
1239
1240

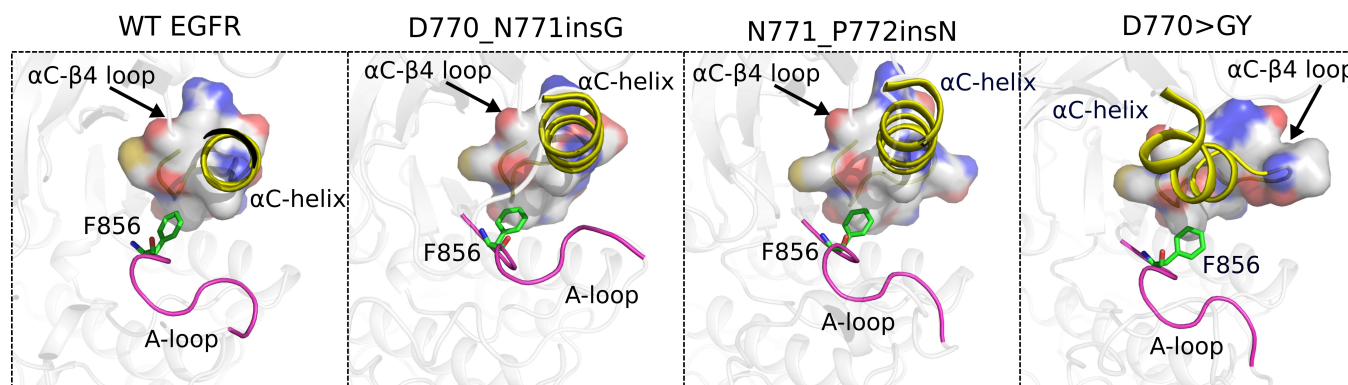


Fig. S10. The alternative inactive state stabilized by activating α C- β 4 loop insertion mutations.

1241
1242
1243
1244
1245
1246
1247
1248
1249
1250
1251
1252
1253
1254
1255
1256
1257
1258
1259
1260
1261
1262
1263
1264
1265
1266
1267
1268
1269
1270
1271
1272
1273
1274
1275
1276
1277
1278
1279
1280
1281
1282
1283
1284
1285
1286
1287
1288
1289
1290
1291
1292
1293
1294
1295
1296
1297
1298
1299
1300
1301
1302

1303
1304
1305
1306
1307
1308
1309
1310
1311
1312
1313
1314
1315
1316
1317
1318
1319
1320
1321
1322
1323
1324
1325
1326
1327
1328
1329
1330
1331
1332
1333
1334
1335
1336
1337
1338
1339
1340
1341
1342
1343
1344
1345
1346
1347
1348
1349
1350
1351
1352
1353
1354
1355
1356
1357
1358
1359
1360
1361
1362
1363
1364

Table S1. The statistics of $\Delta G_{\text{active-inactive}}$ of Fig. 7b.

Phenotype	$\Delta G_{\text{active-inactive}}$ (kJ mol ⁻¹)
WT EGFR	6.02±0.18
D770_N771insG	4.11±0.41
D770>GY	2.45±0.44
N771_P772insN	2.83±0.72

1365
1366
1367
1368
1369
1370
1371
1372
1373
1374
1375
1376
1377
1378
1379
1380
1381
1382
1383
1384
1385
1386
1387
1388
1389
1390
1391
1392
1393
1394
1395
1396
1397
1398
1399
1400
1401
1402
1403
1404
1405
1406
1407
1408
1409
1410
1411
1412
1413
1414
1415
1416
1417
1418
1419
1420
1421
1422
1423
1424
1425
1426

1427
1428
1429
1430
1431
1432
1433
1434
1435
1436
1437
1438
1439
1440
1441
1442
1443
1444
1445
1446
1447
1448
1449
1450
1451
1452
1453
1454
1455
1456
1457
1458
1459
1460
1461
1462
1463
1464
1465
1466
1467
1468
1469
1470
1471
1472
1473
1474
1475
1476
1477
1478
1479
1480
1481
1482
1483
1484
1485
1486
1487
1488

Table S2. Information of all-atom MD simulations performed in the study

Phenotype	State	Length
WT EGFR	Active	1 μ s \times 3
	Inactive	1 μ s \times 3
D770_N771insG	Active	1.5 μ s \times 2
	Inactive	1 μ s \times 4
D770>GY	Active	1 μ s \times 3
	Inactive	1 μ s \times 5
N771_P772insN	Active	1 μ s \times 3
	Inactive	1 μ s \times 5
L704N	Active	1 μ s \times 3
L760R	Active	1 μ s \times 3

1489	1551
1490	1552
1491	1553
1492	1554
1493	1555
1494	1556
1495	1557
1496	1558
1497	1559
1498	1560
1499	1561
1500	1562
1501	1563
1502	1564
1503	1565
1504	1566
1505	1567
1506	1568
1507	1569
1508	1570
1509	1571
1510	1572
1511	1573
1512	1574
1513	1575
1514	1576
1515	1577
1516	1578
1517	1579
1518	1580
1519	1581
1520	1582
1521	1583
1522	1584
1523	1585
1524	1586
1525	1587
1526	1588
1527	1589
1528	1590
1529	1591
1530	1592
1531	1593
1532	1594
1533	1595
1534	1596
1535	1597
1536	1598
1537	1599
1538	1600
1539	1601
1540	1602
1541	1603
1542	1604
1543	1605
1544	1606
1545	1607
1546	1608
1547	1609
1548	1610
1549	1611
1550	1612

Table S3. Information of steered MD (SMD) simulations performed in the study

Simulation	Transition	Collective variable	Spring constant (kJ/mol Å ²)	Length
SMD1	Active to Inactive	All C α RMSD (Residue 701-1017)	10000	10ns
SMD2	Active to Inactive	C α RMSD of α C-helix and A-loop (Residue 756-769 and 855-863)	5000	15ns
SMD3	Inactive to Active	All C α RMSD (Residue 701-1017)	10000	10ns
SMD4	Inactive to Active	C α RMSD of α C-helix and A-loop (Residue 756-769 and 855-863)	5000	15ns

1613	Additional data table S1 (EGFR_Insertion_Mutations.xlsx)	1675
1614	The number of distinct EGFR insertion mutations in COSMIC database v83	1676
1615		1677
1616		1678
1617		1679
1618		1680
1619		1681
1620		1682
1621		1683
1622		1684
1623		1685
1624		1686
1625		1687
1626		1688
1627		1689
1628		1690
1629		1691
1630		1692
1631		1693
1632		1694
1633		1695
1634		1696
1635		1697
1636		1698
1637		1699
1638		1700
1639		1701
1640		1702
1641		1703
1642		1704
1643		1705
1644		1706
1645		1707
1646		1708
1647		1709
1648		1710
1649		1711
1650		1712
1651		1713
1652		1714
1653		1715
1654		1716
1655		1717
1656		1718
1657		1719
1658		1720
1659		1721
1660		1722
1661		1723
1662		1724
1663		1725
1664		1726
1665		1727
1666		1728
1667		1729
1668		1730
1669		1731
1670		1732
1671		1733
1672		1734
1673		1735
1674		1736